Nucleic Acids Research, 1993, Vol. 21, No. 3 657–662

Fine mapping of mitochondrial RNAs derived from the mtDNA region containing a point mutation associated with MELAS

Yasutoshi Koga[1], Mercy Davidson[1], Eric A.Schon[1,2] and Michael P.King[1,*]
Departments of [1]Neurology and [2]Genetics and Development, Columbia University College of Physicians and Surgeons, 630 West 168th Street, New York, NY 10032, USA

Received September 21, 1992; Revised and Accepted December 30, 1992

ABSTRACT

Mitochondrial myopathy, encephalopathy, lactic acidosis, and stroke-like episodes (MELAS) is a mitochondrial disorder associated with heteroplasmic point mutations in the mitochondrial $tRNA^{Leu(UUR)}$ gene. While previous studies have shown that the MELAS mutation at nt-3243 results in impairments in mitochondrial protein synthesis and respiratory chain function, it was not clear whether these were associated with structural alterations in mature RNAs derived from transcription of the region containing the mutation. We have performed fine mapping and high-resolution Northern analysis of RNAs from cybrids derived from two MELAS patients harboring the nt-3243 mutation. No differences in the size or steady-state levels of transcripts from the 16S rRNA, $tRNA^{Leu(UUR)}$, or ND 1 genes (which are contiguous in the mtDNA) were observed between cell lines containing mutated or wild-type mtDNAs. Therefore, it is not likely that the protein synthesis defects observed in cybrids with the MELAS-3243 mutation are directly caused by qualitative alterations in either transcription termination or processing of these mitochondrial RNAs.

INTRODUCTION

MELAS is a maternally-inherited mitochondrial disorder characterized by seizures, lactic acidosis, vomiting, migraine-like headaches, and intermittent cerebral insults resembling strokes and which cause hemiparesis, hemianopia or cortical blindness (1). Most MELAS patients harbor one of two point mutations in the $tRNA^{Leu(UUR)}$ gene of the human mitochondrial genome (2), at mtDNA map positions 3243 (3–5) and 3271 (6). The mutation at nt-3243 is more prevalent in the patient population than is that at nt-3271. The MELAS mutation at nt-3243 is also associated with another disorder, progressive external ophthalmoplegia (7).

The mammalian mitochondrial tRNAs are transcribed as part of larger polycistronic RNAs, in which the tRNA sequences are contiguous or nearly contiguous to the rRNA sequences and the protein-coding sequences. In these polycistronic molecules, the tRNA structures are believed to act as recognition signals for the processing enzymes which make precise endonucleolytic cleavages at the 5′ and 3′ ends of the tRNA sequences in the primary transcripts, yielding the mature rRNAs, mRNAs, and tRNAs. The ribosomal DNA transcription unit, one of three polycistronic transcription units of human mtDNA, terminates at the 3′-end of the 16S rRNA gene just before the $tRNA^{Leu(UUR)}$ gene. This transcript, corresponding to the ribosomal genes, is processed to yield the mature rRNAs and, due to its very high rate of synthesis, is responsible for the bulk of the rRNA formation (8). Transcription termination is mediated by a protein factor which specifically binds within the $tRNA^{Leu(UUR)}$ gene, and which promotes termination of transcription (9,10). The nt-3243 mutation has been shown *in vitro* to impair the binding of this protein factor (10,11) and to affect the efficiency of transcription termination at the end of the 16S rRNA gene (10).

In order to analyze the phenotypic consequences of the MELAS-3243 mutation, we have used a cell culture system which is based upon the repopulation of human cells that are completely devoid of mtDNA, called ϱ° cells, with exogenous mitochondria (12). We repopulated ϱ° cells with mitochondria from two unrelated patients harboring the MELAS-3243 mutation, and created clonal cytoplasmic hybrid (cybrid) cell lines containing different proportions of mutant mtDNAs, including lines with almost 100% mutant mtDNAs (mutant cybrids) and 100% normal mtDNAs (wild-type cybrids) (13). Using genetic, biochemical, and morphological techniques, we found that mutant, but not wild-type cybrids, displayed quantitative deficiencies in cell growth, protein synthesis, and respiratory chain activity (13). Similar results were obtained by others (11).

Transfer hybridization analyses of RNA isolated from the mutant cybrids did not reveal any qualitative or quantitative alterations in either transcription termination at the end of 16S rRNA or in the accuracy of processing of the polycistronic transcript at $tRNA^{Leu(UUR)}$ (13). Unfortunately, errors of a few nucleotides would not have been detected by this method.

* To whom correspondence should be addressed

Similarly, the poor resolution of small RNAs in standard Northern blot analysis precluded any assessment of qualitative or quantitative differences in $tRNA^{Leu(UUR)}$ in these experiments.

In order to analyze whether the MELAS mutation at nt-3243 is associated with errors in transcription termination and processing of the polycistronic transcripts in the region of the mutation, we have performed fine mapping of the mature transcripts derived from the 16S rRNA, $tRNA^{Leu(UUR)}$, and ND 1 genes in both wild-type and mutant cybrids. We also have analyzed the steady-state levels of $tRNA^{Leu(UUR)}$ by high-resolution RNA transfer hybridizations.

MATERIALS AND METHODS

Cell lines

The cell lines used in this study were reported previously (13). They included: 143B206 (ϱ°), 143B (the ϱ^+ parental line of 143B206), wild-type cybrids WS214, WS241, RN236, and RN204, and mutant cybrids WS176, WS216, RN164 and RN223.

Preparation of RNA

Total RNA was isolated from exponentially growing cells by the method of Glison *et al.* (14). For isolation of tRNAs, total cellular RNA (200 μg/lane) was electrophoresed through a 2-mm 5% polyacrylamide-7M urea gel. After electrophoresis, the gel was stained with ethidium bromide, the tRNA region was excised, and the tRNAs were isolated.

Primer extension analyses

The 5′ ends of ND 1 mRNA and $tRNA^{Leu(UUR)}$ were mapped by primer extension analysis. The ND 1 primer was a 21-nt oligonucleotide (Genosys, Houston, TX) corresponding to nt 3494−3474 in the ND 1 gene (see Fig. 2A), radiolabeled at the 5′ terminus with [γ-^{32}P]ATP in the presence of T4 polynucleotide kinase, and purified by elution from a denaturing polyacrylamide gel. Five μg of total RNA was hybridized with 5 pmoles of labeled antisense oligonucleotide ($\sim 3\times10^6$ cpm) in 20 μl of hybridization buffer (40 mM PIPES, pH 6.4, 1 mM EDTA, pH 8.0, 0.4 M NaCl) containing 60% formamide at 37°C overnight. Hybrids were ethanol-precipitated twice and resuspended in 20 ml of reverse transcriptase buffer (50 mM Tris·HCl, pH 7.6, 60 mM KCl, 10 mM $MgCl_2$, 2 mM of each dNTP, 1 mM dithiothreitol, 20 units of placental RNAase inhibitor, and 50 mg/ml actinomycin D). Fifty units of AMV reverse transcriptase (Boehringer Mannheim) were added and the reaction mixture was incubated for 2 h at 42°C. Extension products were ethanol-precipitated twice. A matched sequencing ladder was generated using the same 5′-labeled oligonucleotide as a primer on M13 clone mp19.KR74. This DNA clone contains the 1544 bp *Kpn*I-*Eco*RI fragment of HeLa cell mtDNA (nt 2578−4122) inserted into *Kpn*I-*Eco*RI double-digested M13mp19. Extension products were electrophoresed through an 8% polyacrylamide-7M urea gel and exposed to X-ray film.

A synthetic oligonucleotide corresponding to a 40-nt portion of the $tRNA^{Leu(UUR)}$ gene (sequence 5′-AAGAAGAGGAATTG-AACCTCTGACTGTAAAGGAATAAGTT-3′) was labeled at its 5′ end, gel-purified, and used for primer extension on isolated tRNAs (see Fig. 4A). Five pmoles labeled primer ($\sim 5\times10^6$ cpm) were incubated with 0.5 μg of isolated tRNAs at 95°C for 10 min and then extended in the presence of 5 units of thermostable r*Tth* polymerase (Perkin-Elmer-Cetus) in a DNA thermal cycler (Perkin-Elmer-Cetus) for 35 cycles (1 min at 95°C, 1 min at 60°C), followed by a final extension for 10 min at 60°C. The labeled oligonucleotide was used as a primer to generate a dideoxy sequencing ladder on M13 clone mp19.KR74. Electrophoresis was through an 8% polyacrylamide-7M urea gel.

S1 protection analyses

The 3′ ends of 16S rRNA and $tRNA^{Leu(UUR)}$ and the 5′ end of ND 1 mRNA were mapped by S1 protection analysis. The $tRNA^{Leu(UUR)}$ probe was a synthetic 33-nt oligonucleotide (sequence 5′-GTATGTTGGTGTTAAGAAGAGGAATTGAA-CCTC-3′) end-labeled at the 3′-end with [α-^{32}P] cordycepin-5′-triphosphate (New England Nuclear) in the presence of terminal transferase, and gel-purified (see Fig. 5A). Isolated tRNAs (0.5 μg) were hybridized with ~10 pmoles of labeled probe ($\sim 3\times10^6$ cpm) in 20 μl of hybridization buffer with 35% formamide at 37°C overnight. Total RNA (5 μg) was hybridized with ~10 pmoles of denatured labeled probe in 30 μl of hybridization buffer containing 80% formamide at 45°C overnight. After hybridization, 800 units/ml S1 nuclease (Gibco BRL) in 300 μl S1 buffer (280 mM NaCl, 50 mM sodium acetate, pH 4.5, 4.5 mM $ZnSO_4$, 20 μg/ml salmon sperm DNA) was added and incubated at 37°C for 2 h. S1-protected fragments were electrophoresed through a 10% polyacrylamide-7M urea gel alongside a size ladder generated by partial S1-digestion of the labeled 33-nt oligonucleotide, and the gel was autoradiographed.

The 16S rRNA probe was obtained by gel purification of a 333-bp fragment produced by digestion of a 379-bp PCR fragment (primers spanning nt 3116−3134 and nt 3494−3474) with *Hin*PI, and corresponding to nt 3162−3494 in the mtDNA (see Fig. 1A). The fragment was labeled on the antisense strand by labeling of the 3′ end using [α-^{32}P] dGTP in the presence of Klenow fragment, and then was chased with cold dNTPs. S1-protection, electrophoresis through a 6% polyacrylamide-7M urea gel alongside a dideoxy sequencing ladder, and autoradiography, was as above.

The ND 1 mRNA probe was a 379-bp PCR fragment of mtDNA (nt 3116−3494) obtained by PCR-amplification with the 5′-end-labeled oligonucleotide used in the primer extension analysis of ND 1 in combination with the oligonucleotide corresponding to nt 3116−3134. The resulting fragment was gel-purified and 100 ng was hybridized with 5 μg of total RNA as described above for the ND 1 primer extension analysis. S1-protection, electrophoresis through a 5% polyacrylamide-7M urea gel alongside a matched dideoxy sequencing ladder, and autoradiography, was as above.

High-resolution RNA transfer hybridization analyses of mitochondrial tRNAs

Total RNA (5 μg/lane) was electrophoresed through 0.75-mm 20% polyacrylamide-7M urea gels under highly-denaturing (40 V/cm without cooling) or less-denaturating (10V/cm at 4°C) conditions. The tRNA region of the gel was transferred electrophoretically onto a Zeta-Probe GT membrane (Bio-Rad) using a Trans-Blot SD apparatus (Bio-Rad) according to the manufacturer's recommendations.

Mitochondrial tRNAs were detected by hybridization to specific mtDNA probes. For detection of $tRNA^{Leu(UUR)}$ we used 2 *Mse*I mtDNA fragments comprising most of the $tRNA^{Leu(UUR)}$ gene (nt 3232−3264 and nt 3265−3291). For detection of $tRNA^{Val}$ we used an *Mse*I mtDNA fragment within the $tRNA^{Val}$ gene (nt

1614−1653). Both probes were obtained by *Mse*I digestion of an appropriate PCR-amplified fragment, followed by gel isolation and self-ligation to increase the size of the probe; labeling was by random-priming (15). For detection of $tRNA^{Lys}$, 10 pmoles of a synthetic oligonucleotide corresponding to a region within the $tRNA^{Lys}$ gene (nt 8321−8299) were 5′-end labeled and purified by ethanol precipitation. The hybridizations were performed for 12 h in 6×SSC, 3×Denhardt's solution, 1% SDS, 10% PEG, and 1 mg/ml denatured salmon sperm DNA containing the labeled probe (~5×10^6 cpm/ml at a specific activity of ~10^8 cpm/μg). Hybridization was at 45°C for $tRNA^{Lys}$ and at 50°C for $tRNA^{Leu(UUR)}$ and $tRNA^{Val}$. After hybridization, the filters were washed in 1×SSC, 1% SDS at the same temperature as that used for hybridization, and then autoradiographed at −70°C with an intensifying screen. Signals obtained from each probe were analyzed quantitatively by densitometry with a Molecular Dynamics 300A computing densitometer. Each probe was hybridized sequentially after stripping off the previous probe by boiling in 0.1×SSC, 0.5% SDS for 1 h.

RESULTS AND DISCUSSION

Mapping of the 3′ end of 16S rRNA

In order to determine if transcription termination was occurring correctly at the 3′ end of the ribosomal DNA region, the 3′ ends of the 16S rRNA transcripts in normal and mutant cybrids were mapped by S1 nuclease protection (Fig. 1A). A 333-nt 3′-end-labeled probe which was complementary to sequences spanning the 3′ end of 16S rRNA (68 nt), all of $tRNA^{Leu(UUR)}$ (75 nt), and the 5′ end of the ND 1 (190 nt) genes was hybridized to total RNA isolated from mutant and wild-type cybrids and was subsequently digested with S1 nuclease. This fragment protected RNA fragments of three main sizes (Fig. 1B). The largest fragment ('a' in Fig. 1B) was derived from protection of the full-length 333-nt probe. Significantly, the intensity of the signal was much stronger in mutant cybrids than that in wild type cybrids or in the 143B control, implying that these fragments were derived from S1 protection of RNA 19. RNA 19 is a minor RNA transcript corresponding to the 16S rRNA, $tRNA^{Leu(UUR)}$, and ND 1 genes (i.e., no processing occurs at the $tRNA^{Leu(UUR)}$ gene) which is present at higher steady-state levels in the mutant cybrids (13). Size group 'b' migrated at 110−114 nt, corresponding to an AT-rich region in the middle of the $tRNA^{Leu(UUR)}$ gene at nt 3271−3275. Presumably, the RNA:DNA hybrid was not completely stable in this region and some hybrids were susceptible to S1 nuclease digestion. No protected fragments corresponding to 16S rRNA + $tRNA^{Leu(UUR)}$ were observed.

The smallest size group ('c' in Fig. 1B) was composed of fragments 66−68 nt in length, corresponding to the distance from 3′ end of the probe to nt 3227−3229 at the 3′ end of the 16S rRNA gene. There was no significant difference in the size or amount of the protected fragments in RNA from mutant and wild type cybrids. These results are similar to those reported by Dubin *et al.* (16), who found that HeLa cell 16S rRNA contains two major transcription termini, corresponding in the mtDNA sequence to nucleotides 3228 and 3229, which are immediately before the $tRNA^{Leu(UUR)}$ gene.

The MELAS-3243 mutation also occurs in a DNA region that may be responsible for the specific termination of transcription at the end of the rRNA genes (9, 10). This mutation has been shown *in vitro* to impair the proper termination of transcription at the end of the 16S rRNA gene, by altering the binding of a protein factor that promotes this termination (10, 11). If termination does not occur, rRNA transcription should continue on the heavy strand, which also encodes 12 of the 13 mitochondrial polypeptides. Analyses of the steady-state levels of mitochondrial transcripts have not revealed any significant differences in the steady-state levels or in the ratios of rRNAs and mRNAs either *in vivo* or in cell culture systems (11, 13, 17, 18). The evidence reported here of multiple 3′ termini of 16S rRNA molecules, each of which is present at identical levels in both the mutant and the wild-type cybrids, suggests that the vast majority of 16S rRNA molecules are derived from transcription of the rRNA genes with transcription termination occurring at the 3′ end of the 16S rRNA. If high levels of transcription were occurring beyond the normal transcription

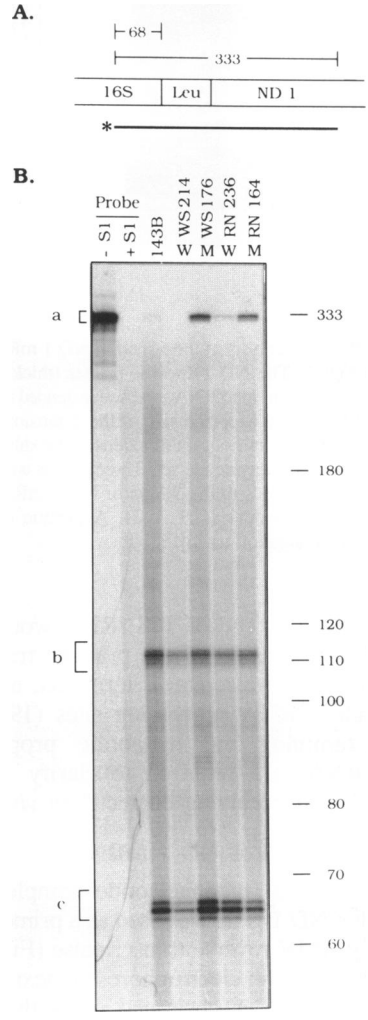

Figure 1. S1-protection analysis of the 3′ end of 16S rRNA transcripts. **A.** Analytical scheme. Sizes of the full-length probe and the expected S1-protected region in 16S rRNA are indicated above the map. The 333-nt probe (thick line) labeled at the 3′ end (asterisk) was annealed to total RNA, followed by S1 digestion. **B.** Autoradiogram of S1-protected products electrophoresed through a 6% denaturing polyacrylamide gel. Three groups of protected fragments are indicated, corresponding to the full-length probe (a), an AT-rich region at nt 3271−3275 in the $tRNA^{Leu(UUR)}$ gene (b), and the 3′ region of 16S rRNA (c). Sizes are right are from a dideoxy sequencing ladder. Wild-type (W), mutant (M), and 143B ϱ^+ cell lines are described in Ref. 13.

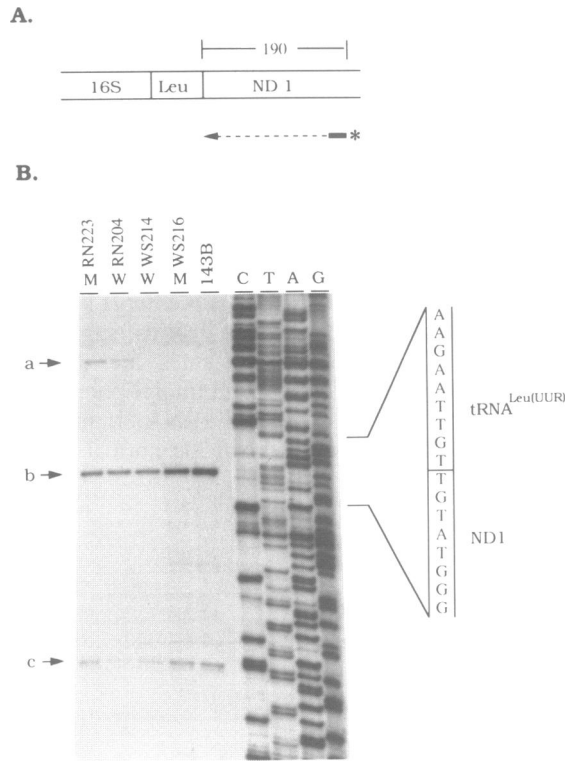

Figure 2. Primer extension analysis of the 5′ end of ND 1 mRNA. **A.** Analytical scheme. Map as in Fig. 1. The ND 1-specific primer (thick line) labeled at its 5′ end (asterisk) was annealed to total RNA, and was extended using AMV reverse transcriptase (dotted line). The expected size of the extension product, in nt, is shown above the map. **B.** Autoradiogram of extension products electrophoresed through an 8% denaturing polyacrylamide gel. Three signals were observed (a–c). The major signal (b) corresponds to the 5′ end of ND 1 mRNA (arrow), based on the matched sequencing ladder (C,T,A,G). A portion of the sequence is expanded at right. Other notation as in Fig. 1.

termination sites, the 3′ end of 16S rRNA would be expected to be formed by processing of the primary transcript, which would result in a single discrete 3′ terminus, as occurs at the other mitochondrial RNA processing sites (19, 20). Further experiments examining the metabolic properties of the mitochondrial RNAs are required to clarify if transcription termination is indeed occurring correctly *in vivo*.

Mapping of the 5′ end of ND 1 mRNA

A 5′-end-labeled 21-nt oligonucleotide complementary to nt 3494–3474 in the ND 1 gene was used as a primer for extension on total RNA by AMV reverse transcriptase (Fig. 2A). Primer extension products were electrophoresed next to a matched dideoxy sequencing ladder generated using the same labeled primer. Three main extension products were observed (Fig. 2B). The most intense fragment ('b' in Fig. 2B) was 190 nt long, and corresponded exactly to the 5′ end of ND 1 mRNA at nt-3305, immediately 3′ to the last base of the $tRNA^{Leu(UUR)}$ gene. This position was identical to the 5′ terminus found for ND 1 mRNA in HeLa cells (19). There was no significant difference in the size or amount of this product between wild-type or mutant cybrids.

Two other extension products were also observed. Fragment 'c' was a 'strong-stop' product located within the ND 1 mRNA at nt-3358. Fragment 'a' was a product approximately 246 nt long, and was presumed to be derived from extension of the primer on an unprocessed RNA template. No extension products mapping to the 5′ end of $tRNA^{Leu(UUR)}$ were detected in either the mutant or the wild-type cybrids (data not shown).

S1 protection analysis of the 5′ end of the ND 1 mRNA was also performed. A 379-bp fragment of mtDNA corresponding to nt 3116–3494, 5′-end-labeled on the antisense strand, was hybridized with total RNA isolated from mutant and wild-type cybrids and was subsequently digested with S1 nuclease (see Materials and Methods). The major protected fragment, 190 nt long, corresponded exactly to the 5′ end of the ND 1 mRNA at nt-3305, and was identical to that observed in the primer extension analysis (data not shown). No protected fragments corresponding to fragment 'a' or fragment 'c' were present. This would indicate that these two fragments originated through strong stops in the reverse transcription reaction and do not correspond to authentic 5′ ends of mitochondrial RNA species.

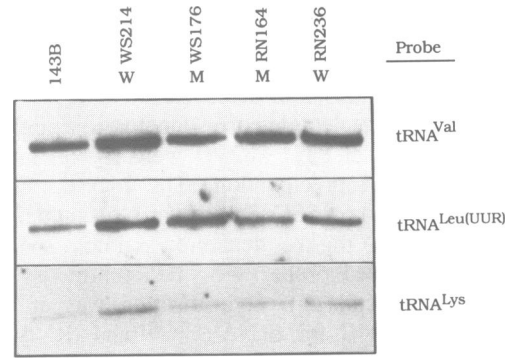

Figure 3. High resolution RNA transfer hybridization analysis of mitochondrial tRNAs. Autoradiogram of a Northern hybridization of total RNA electrophoresed under highly denaturing conditions. Probes are indicated at right. Other notation as in Fig. 1.

High-resolution RNA transfer hybridization analysis of mitochondrial tRNAs

In order to determine whether the size or steady-state levels of $tRNA^{Leu(UUR)}$ differed between mutant and wild-type cybrids, we performed high-resolution RNA transfer hybridization analysis of total RNAs isolated from mutant and wild-type cybrids. Under highly denaturing electrophoretic conditions, the $tRNA^{Leu(UUR)}$ probe detected a single band in all the cybrids examined (Fig. 3), which we presume corresponds to mature, fully-processed $tRNA^{Leu(UUR)}$. Single hybridizing bands were also observed when labeled $tRNA^{Val}$ or $tRNA^{Lys}$ DNAs were used as probes; the migration of these bands in the gel relative to that of $tRNA^{Leu(UUR)}$ corresponded to the differences in the expected sizes of these tRNAs (2), and there was no apparent difference in the electrophoretic mobility of these species between wild-type and mutant cybrids. Densitometry of the autoradiograms showed that there were no significant differences between mutant and wild-type cells in the relative steady-state levels of $tRNA^{Val}$, $tRNA^{Leu(UUR)}$ and $tRNA^{Lys}$.

Under less denaturing electrophoretic conditions (see Materials and Methods), using $tRNA^{Leu(UUR)}$ DNA as a probe, we

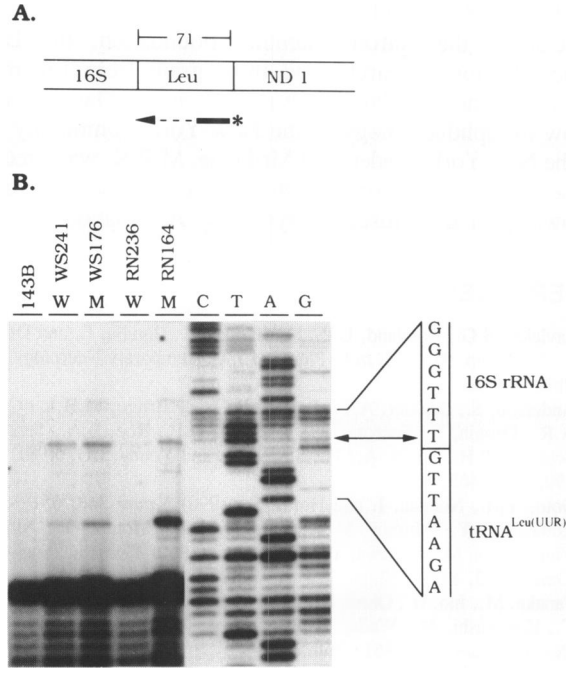

Figure 4. Primer extension analysis of the 5′ end of tRNA$^{Leu(UUR)}$. **A.** Analytical scheme. Map as in Fig. 1. The tRNA$^{Leu(UUR)}$-specific primer (thick line) labeled at its 5′ end (asterisk) was annealed to isolated tRNAs, and was extended using r*Tth* thermostable polymerase (dotted line). The expected size of the extension product, in nt, is shown above the map. **B.** Autoradiogram of extension products electrophoresed through an 8% denaturing polyacrylamide gel. The major signal corresponds to extension one nucleotide 5′-upstream of the starting nucleotide of tRNA$^{Leu(UUR)}$ (arrow) according to the matched dideoxy sequencing ladder (C,T,A,G). Other notation as in Fig. 1.

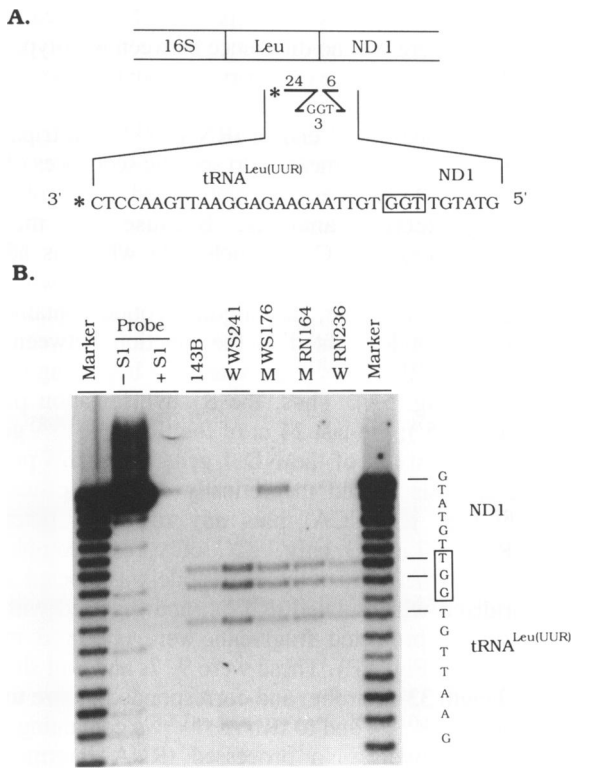

Figure 5. S1 analysis of the 3′ end of tRNA$^{Leu(UUR)}$. **A.** Analytical scheme. A map of the 16S rRNA/tRNA$^{Leu(UUR)}$/ND 1 region of human mtDNA is shown. The 33-nt 'tripartite' probe (thick lines; numbers indicate lengths, in nt, of the tRNA- and ND 1-derived segments) labeled at the 3′ end (asterisk), contained a 3-nt mismatched region ('triangular' and boxed regions) corresponding to the complement of -CCA which is added posttranscriptionally to the 3′ end of tRNA$^{Leu(UUR)}$. This probe was annealed to isolated tRNAs, followed by S1 digestion. **B.** Autoradiogram of S1-protected products electrophoresed through a 10% denaturing polyacrylamide gel. Protected signals are indicated at right, as is the complementary DNA sequence of the region. Markers are partial S1-digestion products of the 33-nt probe, corresponding to the oligonucleotide regions and sequence shown at right. Controls with (+S1) and without (−S1) S1 nuclease are shown. Other notation as in Fig. 1.

observed 2 hybridizing bands in the wild-type cybrids and 4 bands in the mutant cybrids (data not shown). The slight migration differences of tRNA$^{Leu(UUR)}$ that were observed between wild-type and mutant cybrids under the less denaturing conditions may reflect the change from A to G at nt-3243 in the primary sequence of the tRNA. Additionally, differences in posttranscriptional modifications or the potential for wild-type and mutant tRNAs to adopt slightly different secondary or tertiary structures under these conditions of analysis may also have contributed to the observed mobility differences. Using a third system for electrophoretic analysis, both wild-type and mutant tRNA$^{Leu(UUR)}$ were found to migrate identically and as a single species (11).

Fine-mapping of tRNA$^{Leu(UUR)}$

In order to confirm that tRNA$^{Leu(UUR)}$ was in fact a single uniform species, a fine-mapping analysis of this tRNA was undertaken. The 5′ end of tRNA$^{Leu(UUR)}$ was examined by primer extension analysis. A 5′-end-labeled 40-nt oligonucleotide complementary to nt 3300−3261 in the tRNA$^{Leu(UUR)}$ gene (Fig. 4A) was used as a primer for extension on isolated tRNAs in the presence of thermostable r*Tth* polymerase. Primer extension products were electrophoresed in parallel to a dideoxy sequencing ladder, using the same labeled oligonucleotide as a primer (Fig. 4B). The major primer extension product was 72 nt long; the 5′ end mapped to nt-3229, which is located 1 nt upstream of the presumed 5′ end of tRNA$^{Leu(UUR)}$. A 'strong-stop' signal located near nt-3238 within tRNA$^{Leu(UUR)}$, as well as two fainter signals mapping 7 and 8 nt upstream of tRNA$^{Leu(UUR)}$ (presumably at nt-3222 and nt-3223 within 16S rRNA), were also observed. Primer extension of total RNA using AMV reverse transcriptase showed major extension products that mapped to the expected 5′ end of tRNA$^{Leu(UUR)}$ as well as to 2−3 nt upstream of the starting nucleotide of tRNA$^{Leu(UUR)}$ (data not shown).

It is not known whether the slightly longer-than-expected 5′-extension products were derived from the actual 5′-end of the tRNA$^{Leu(UUR)}$ transcript, or were due to artifacts of the reverse transcriptase reaction during elongation. It has been reported that reverse transcription of a full-length mRNA adds one or more bases to the authentic 5 ' end of the template (21). Because the templates for primer extension in the experiments using *Tth* polymerase were size-fractionated tRNA, these longer extension products are unlikely to be derived from extension on RNA 19. The possibility exists that they may be related to the minor hybridization signals observed in the tRNA hybridization analysis under less denaturing conditions. Sequence analysis of

$tRNA^{Leu(UUR)}$ may clarify these discrepancies. Nevertheless, in both experiments, there was no difference between wild-type and mutant cybrids in either the size or apparent amounts of the primer extension products.

In order to examine the 3′ end of $tRNA^{Leu(UUR)}$, a tripartite 33-nt oligonucleotide complementary to specific sequences of the $tRNA^{Leu(UUR)}$ and ND 1 genes was synthesized as a probe for S1 nuclease protection analysis. Because the mature $tRNA^{Leu(UUR)}$ contains a -CCA trinucleotide which is added post-transcriptionally to the 3′ end of the tRNA, and which is not found in the tRNA gene, the oligonucleotide contained a 3′-GGT-5′ trinucleotide located at the junction between the expected 3′ end of $tRNA^{Leu(UUR)}$ gene and the beginning of the ND 1 gene (see Fig. 5A). Thus, the S1 hybridization probe consisted of (3′ to 5′): the last 24 nt of the $tRNA^{Leu(UUR)}$ gene, GGT, and the first six nt of the ND 1 gene. With this probe, S1 nuclease analysis should theoretically detect unprocessed $tRNA^{Leu(UUR)}$ (i.e. no -CCA) plus any of the 3 potential processed tRNAs (i.e. -C only, -CC only, and completely processed -CCA). When this oligonucleotide was labeled at its 3′ end, hybridized with isolated tRNAs, and digested with S1 nuclease, 3 major protected fragments were observed in all analyzed cell lines (Fig. 5B). These were 9, 7, and 6 nt shorter than the full length 33-nt probe, and corresponded in size to the unmodified $tRNA^{Leu(UUR)}$ and to $tRNA^{Leu(UUR)}$s containing -CC and -CCA, respectively. No processed tRNA intermediate containing only -C was observed. There was no difference in the size or apparent amounts of these fragments between wild-type and mutant cybrids. These data contrast with our data obtained by high-resolution RNA transfer hybridization analysis, in which a single tRNA species of uniform length was observed. Presumably, the multiple bands observed in the S1 analysis were due to breathing at the ends of the oligonucleotide in the RNA:DNA hybrids and subsequent digestion by S1 nuclease. Alternatively, but less likely, multiple RNA species of identical length and corresponding to $tRNA^{Leu(UUR)}$ are present in mitochondria, in which these species are offset at their 5′ and 3′ ends by a single nucleotide.

CONCLUDING REMARKS

The results presented here imply that the mutation at nt-3243 has no effect *in vivo* on the accuracy of transcription termination at the end of the ribosomal RNA genes, on the precise endonucleolytic cleavage of the polycistronic RNA at $tRNA^{Leu(UUR)}$, or on the postranscriptional addition of -CCA at the 3′ end of $tRNA^{Leu(UUR)}$. While the A → G transition at nt-3243 does not appear to affect the accuracy of RNA processing, quantitative differences in processing at $tRNA^{Leu(UUR)}$ have been observed (13). The increased amounts of the transcript corresponding to the 16S rRNA + $tRNA^{Leu(UUR)}$ + ND 1 genes (i.e. RNA 19) found in mutant cybrids clearly demonstrate that RNA processing is not occurring in mutant cybrids as efficiently as in wild-type cybrids. While the reasons for this are unknown, we believe that elevated levels of RNA 19 may play an important role in the pathogenesis of this disorder (13,22).

ACKNOWLEDGMENTS

We thank C.T.Moraes and S.DiMauro for critical comments, and J.Sadlock and J.Rogers for expert technical assistance. This work was supported by grants from the National Institutes of Health (NS28828 and AG08702), the Muscular Dystrophy Association, the Aaron Diamond Foundation, the Eppley Foundation for Research, and by a grant from Libero and Graziella Danesi (Milano, Italy). Y.K. is the David Warfield Fellow in Ophthalmology of the New York Community Trust and the New York Academy of Medicine. M.P.K. was a recipient of the Harry Zimmerman Neuromuscular Disease Research Fellowship of the Muscular Dystrophy Association.

REFERENCES

1. Pavlakis, S.G., Rowland, L.P., DeVivo, D.C., Bonilla, E. and DiMauro, S. (1988). pp. 95–133. *In* F. Plum (ed.), Contemporary Neurology, Davis, Philadelphia.
2. Anderson, S., Bankier, A.T., Barrell, B.G., de Bruijn, M.H.L., Coulson, A.R., Drouin, J., Eperon, I.C., Nierlich, D.P., Roe, B.A., Sanger, F., Schreier, P.H., Smith, A.J.H., Staden, R. and Young, I.G. (1981) *Nature* **290,** 457–465.
3. Goto, Y.-i., Nonaka, I. and Horai, S. (1990) *Nature* **348,** 651–653.
4. Kobayashi, Y., Momoi, M.Y., Tominaga, K., Momoi, T., Nihei, K., Yanagisawa, M., Kagawa, Y. and Ohta, S. (1990) *Biochem. Biophys. Res. Comm.* **173,** 816–822.
5. Tanaka, M., Ino, H., Ohno, K., Ohbayashi, T., Ikebe, S., Sano, T., Ichiki, T., Kobayashi, M., Wada, Y. and Ozawa, T. (1991) *Biochem. Biophys. Res. Commun.* **174,** 861–868.
6. Goto, Y.-i., Nonaka, I. and Horai, S. (1991) *Biochim. Biophys. Acta* **1097,** 238–240.
7. Moraes, C.T., Ciacci, F., Silvestri, G., Shanske, S., Sciacco, M., Hirano, M., Schon, E.A., Bonilla, E. and DiMauro, S. (1992), *Neuromuscular Disorders*, In Press.
8. Montoya, J., Gaines, G.L. and Attardi, G. (1983) *Cell* **34,** 151–159.
9. Kruse, B., Narasimhan, N. and Attardi, G. (1989) *Cell* **58,** 391–397.
10. Hess, J.F., Parisi, M.A., Bennett, J.L. and Clayton, D.A. (1991) *Nature* **351,** 236–239.
11. Chomyn, A., Martinuzzi, A., Yoneda, M., Daga, A., Hurko, O., Johns, D., Lai, S.T., Nonaka, I., Angelini, C. and Attardi, G. (1992) *Proc. Natl. Acad. Sci. USA* **89,** 4221–4225.
12. King, M.P. and Attardi, G. (1989) *Science* **246,** 500–503.
13. King, M.P., Koga, Y., Davidson, M. and Schon, E.A. (1992) *Mol. Cell Biol.* **12,** 480–490.
14. Glison, V., Crkvenjakov, R. and Byus, C. (1974) *Biochemistry* **13,** 2633–2637.
15. Feinberg, A. and Vogelstein, B. (1983) *Anal. Biochem.* **132,** 6–13.
16. Dubin, D.T., Montoya, J., Timko, K.D. and Attardi, G. (1982) *J. Mol. Biol.* **157,** 1–19.
17. Moraes, C.T., Ricci, E., Bonilla, E., DiMauro, S. and Schon, E.A. (1992) *Am. J. Hum. Genet.* **50,** 934–949.
18. Hammans, S.R., Sweeney, M.G., Wicks, D.A.G., Morgan-Hughes, J.A. and Harding, A.E. (1992) *Brain* **115,** 343–365.
19. Montoya, J., Ojala, D. and Attardi, G. (1981) *Nature* **290,** 465–470.
20. Ojala, D., Montoya, J. and Attardi, G. (1981) *Nature* **290,** 470–474.
21. Shelness, G.S. and Williams, D.L. (1985) *J. Biol. Chem.* **260,** 8637–8646.
22. Schon, E.A., Koga, Y., Davidson, M., Moraes, C.T. and King, M.P. (1992) *Biochim. Biophys. Acta* 1101, 206–209.